Energy and momentum relaxation of two-dimensional electron gas due to near-surface deformation scattering

V. I. Pipa and F. T. Vasko
Institute of Semiconductor Physics, Kiev, 252650, Ukraine

V. V. Mitin[a)]
Department of Electrical and Computer Engineering, Wayne State University, Detroit, Michigan 48202

(Received 30 January 1998; accepted for publication 9 November 1998)

We model the influence of a cap layer with a fixed thickness placed on top of a semi-infinite heterostructure on the energy and momentum relaxation rates for two-dimensional electrons localized in the lowest subband of a quantum well, and interacting with the acoustic phonon via the deformation potential. The relaxation rates are derived from the corresponding balance equations for a small deviation from the thermodynamic equilibrium. Our results indicate that at low temperatures the efficiency of the scattering is changed substantially depending on the mechanical conditions at the surface; the cases of free and rigid surfaces are considered. The dependencies of the electron energy and momentum rates on the distance from the electron layer to the surface, on the temperature and electron concentration are analyzed. It is shown that the efficiencies of relaxation are changed substantially (up to two times for standard parameters of GaAs or InAs based quantum wells) depending nonmonotonically on the distance of the 2D layer to the surface and on the electron temperature. © *1999 American Institute of Physics.* [S0021-8979(99)03004-2]

I. INTRODUCTION

It is usually accepted that the modifications of near-surface phonon modes do not change the scattering of two-dimensional 2D electrons by acoustic phonons substantially; they contribute to the scattering rates only correction factors of the order of unity.[1,2] This is why it has been possible to explain the measured temperature dependencies of the mobility[3] and energy losses[4,5] based on theories[6,7] using conventional 3D bulk phonon modes. However, in the case of low temperatures, the effect of acoustic phonons confinement on electron transport is well pronounced in free-standing heterostructures[8] as well as in the energy relaxation of 2D electrons placed near a free[9] or rigid[10] surface. In recent theoretical work,[11] a substantial contribution of thermally excited surface acoustic phonons to the transport relaxation rate was obtained. To understand the peculiarities of near-surface electron–acoustic–phonon scattering, let us consider the behavior of the energy of the electron–phonon deformation interaction, $D\,\mathrm{div}\,\mathbf{u}$, near a free or clamped boundary as depicted in Fig. 1; here D is the deformation potential constant, and $\mathbf{u}$ is a vector of displacement. In the latter case, the displacement components are equal to zero at the boundary and their normal derivatives are not constrained. For a free surface, normal components of the stress tensor vanish at the boundary, while the displacements are not constrained. Hence, $D\,\mathrm{div}\,\mathbf{u}$ is enhanced near a clamped surface and suppressed near a free surface. As for typical heterostructures, the width of a layer between the quantum well and the surface is compared to the characteristic wavelengths of phonons which contribute the scattering; thus, the near-surface modification of the acoustic field depends on the mechanical boundary conditions and will effect the electron–phonon interaction. In the case when the acoustic wavelengths are comparable with the width of the electron layer, the efficiency of electron–phonon interaction may be enhanced near a rigid boundary and suppressed near a free boundary. Besides this modification—which can either enlarge or suppress electron–phonon interaction—near-surface scattering probabilities are always augmented by the transformation of the incident transverse acoustic waves into the decaying longitudinal waves as well as by the contribution of Rayleigh waves: these waves exist in a medium with free surfaces (since they are related with a deviation of the boundary from a plane) and they are absent in one with the rigid surfaces.

The partial contributions of these additional scattering mechanisms are quite different for the temperature ranges determined by the characteristic temperatures:[9]

$$T_0 = 2s_l p_F, \quad T_1 = 2s_l \hbar/d, \tag{1}$$

where s_l is the velocity of the longitudinal phonons, p_F is Fermi momentum, d is a characteristic width of 2D layer; here the temperature is measured in energy units. In the temperature range $T > T_1$, the scattering processes are quasielastic, the phonon distribution may be considered as the equipartition, the surface effect appeared to be small, and the usual ''bulk phonon'' results for a mobility and energy relaxation rate[6,7] of 2D electrons are appropriate. The noticeable surface effects on the energy losses which were predicted theoretically in Refs. 9 and 10 for the intermediate temperature range ($T_0 \ll T \ll T_1$), may be realized only in narrow 2D layers with low electron density. Near-surface modifications of the energy losses and momentum relaxation may be significant for low temperatures with the small-angle

[a)]Electronic mail: mitin@ece6.eng.wayne.edu

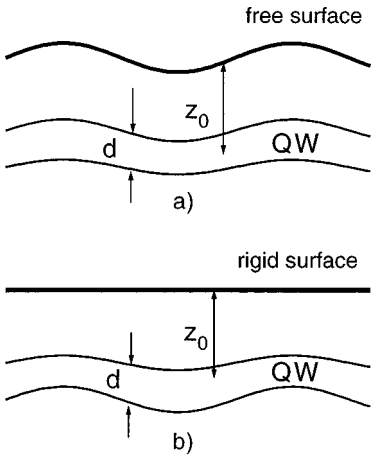

FIG. 1. Schematic of the structure under consideration and the modification of QW's vibrations near (a) free and (b) rigid surfaces.

inelastic scattering events, i.e., for $T \sim T_0$ (Bloch–Grüneisen regime). As a result, the relaxation rates due to the total scattering at all types of phonons may be as suppressed as enhanced in comparison with the bulk case depending on above-mentioned factors.

As far as we know, a detailed study of the surface effect on the electron energy and momentum relaxation has not been carried out previously, and in this article we present calculations of the energy and momentum relaxation rates of electrons within the lowest subband of a quantum well due to scattering by acoustic phonon modes of a semi-infinite sample via the deformation potential. The transition probability is obtained for the cases of both a free and a rigid surface. The relaxation rates are derived from the corresponding balance equations in the case of a small deviation from thermodynamic equilibrium, i.e., when a temperature increase is small compared with its equilibrium value or a drift velocity is small compared to the Fermi velocity. The analysis of the dependencies of the relaxation rates on the temperature, on the width of a top layer and on the electron concentration for the two kinds of boundary conditions are given. Employing the same boundary conditions, we have also studied the energy losses of hot 2D electrons, where the temperature substantially exceeds the lattice temperature. The results obtained for this case are presented in a separate paper,[12] and we do not include them in this article.

In Sec. II we evaluate the transition probabilities for the cases of free and clamped surfaces. The expressions for the energy and momentum relaxation rates are determined in Sec. III. In Sec. IV we analyze the asymptotic expressions for these relaxation rates. The numerical results concerning the low-temperature range, where the effect under consideration may be large, are presented in Sec. V. Discussion and concluding remarks are given in Sec. VI.

II. PROBABILITY OF TRANSITIONS

The transition probability from the electron state $\psi_{\mathbf{p}}(\mathbf{r})$ with 2D momentum $\mathbf{p}$ ($\mathbf{r}$) is three-dimensional coordinate) to the state $\psi_{\mathbf{p}'}(\mathbf{r})$ with momentum $\mathbf{p}'$ due to the interaction of an electron with acoustic phonon modes via deformation potential is given by[9]

$$W(\mathbf{p},\mathbf{p}') = \left(\frac{D}{\hbar}\right)^2 \int d\mathbf{r} \int d\mathbf{r}'\, \psi_{\mathbf{p}'}(\mathbf{r})^* \psi_{\mathbf{p}'}(\mathbf{r}')\psi_{\mathbf{p}}(\mathbf{r})\psi_{\mathbf{p}}(\mathbf{r}')^* \times \langle (\nabla \hat{\mathbf{u}}_{\mathbf{r}})(\nabla' \hat{\mathbf{u}}_{\mathbf{r}'}) \rangle. \tag{2}$$

Here D is the deformation potential constant, $\hat{\mathbf{u}}_{\mathbf{r}}$ is the operator of the phonon displacement field, $\langle ... \rangle$ denotes the statistical average over an equilibrium phonon distribution at a lattice temperature T. The correlator $\langle \hat{u}^{\alpha}_{\mathbf{r}} \hat{u}^{\beta}_{\mathbf{r}'} \rangle$, where $\alpha,\beta = x,y,z$, can be expressed in terms of the Green's function of elasticity theory, $G^{\alpha\beta}_{\omega}(\mathbf{r},\mathbf{r}')$, in the following form:[13]

$$\langle \hat{u}^{\alpha}_{\mathbf{r}} \hat{u}^{\beta}_{\mathbf{r}'} \rangle = -2\hbar\, \mathrm{Im}\, G^{\alpha\beta}_{\omega+i0}(\mathbf{r},\mathbf{r}') \begin{cases} (N_{\hbar\omega/T}+1) \\ N_{\hbar\omega/T} \end{cases}, \tag{3}$$

where $N_{\hbar\omega/T} = [\exp(\hbar\omega/T)-1]^{-1}$ is the Planck distribution function, and the energy of a phonon, $\hbar\omega$, is related to electron energies of the initial and final states (ϵ and ϵ') by the energy conservation law. The upper phonon occupation factor corresponds to emission processes and the lower one to absorption processes.

We will consider 2D electron gas placed in a bounded medium ($z \geqslant 0$) parallel to the surface plane xy; see Fig. 1. Due to translation invariance in this plane, to calculate $W(\mathbf{p},\mathbf{p}')$ one has to know the Fourier transformation of retarded Green's function in 2D plane, $G^{\alpha\beta}_{\omega q}(z,z')$. Here the 2D wave vector $\mathbf{q}$ is related to $\mathbf{p}$ and $\mathbf{p}'$ by the momentum conservation law, so that $G^{\alpha\beta}_{\omega q}$ depends on

$$\hbar\omega = |\epsilon - \epsilon'|, \quad \hbar q = |\mathbf{p} - \mathbf{p}'|. \tag{4}$$

Assuming the structure under consideration to be an isotropic elastic continuum, we can use $\mathbf{q}=(q,0)$ so that the Green's function will be determined from the equation:

$$\begin{bmatrix} s_t^2 \frac{d^2}{dz^2} - (s_l q)^2 + \omega^2 & (s_l^2 - s_t^2) iq \frac{d}{dz} \\ (s_l^2 - s_t^2) iq \frac{d}{dz} & s_l^2 \frac{d^2}{dz^2} - (s_t q)^2 + \omega^2 \end{bmatrix} \times \begin{bmatrix} G^{xx}_{\omega q}(z,z') & G^{xz}_{\omega q}(z,z') \\ G^{zx}_{\omega q}(z,z') & G^{zz}_{\omega q}(z,z') \end{bmatrix} = \frac{\hat{1}}{\rho}\delta(z-z'), \tag{5}$$

where s_t is the transverse velocity of sound, ρ is the density of the semiconductor, and $\hat{1}$ is the identity matrix. If we neglect the differences between the mechanical parameters of the heterostructure's materials, the system Eq. (5) may be solved with the boundary conditions at the sample's surfaces. Boundary conditions at $z=0$ are given by

$$G^{\alpha\beta}_{\omega q}(z=0,z') = 0, \tag{6}$$

for a clamped surface and

$$\begin{cases} \left(\frac{dG^{xx}_{\omega q}}{dz} + iqG^{zx}_{\omega q} \right)_{z=0} = 0 \\ \left[\frac{dG^{zx}_{\omega q}}{dz} + iq(1-2\lambda)G^{xx}_{\omega q} \right]_{z=0} = 0 \end{cases}$$

$$\begin{cases} \left[\dfrac{dG^{zz}_{\omega q}}{dz}+iq(1-2\lambda)G^{xz}_{\omega q}\right]_{z=0}=0 \\ \left(\dfrac{dG^{xz}_{\omega q}}{dz}+iqG^{zz}_{\omega q}\right)_{z=0}=0 \end{cases} \tag{7}$$

for a free surface; here we have introduced $\lambda=(s_t/s_l)^2$. Conditions [Eq. (6)] correspond to the displacement $\mathbf{u_r}$ vanishing at $z=0$, while Eq. (7) ensures the absence of a normal stress at $z=0$. Assuming the structure to be thick, the boundary condition at the back surface are replaced by exponentially decaying or outgoing wave conditions at $z\to\infty$.

Excluding longitudinal electron coordinates from Eq. (2), we obtain the transition probabilities for emission and absorption phonon processes in the form

$$W(\mathbf{p},\mathbf{p}')=\frac{2D^2}{\hbar L^2}\int dz\,\varphi_z^2\int dz'\,\varphi_{z'}^2 K_{\omega,q}(z,z') \times\begin{cases}(N_{\hbar\omega/T}+1) & \epsilon>\epsilon' \\ N_{\hbar\omega/T} & \epsilon<\epsilon'\end{cases}, \tag{8}$$

where emission and absorption correspond to the upper and lower factors, respectively. Here, φ_z is the wave function of an electron in the lowest subband, L^2 is the normalized area in plane xy, and the kernel $K_{\omega,q}(z,z')$ is given by

$$K_{\omega,q}(z,z')=-\mathrm{Im}\left(q^2G^{xx}_{\omega q}-iq\frac{\partial G^{zx}_{\omega q}}{\partial z}+iq\frac{\partial G^{xz}_{\omega q}}{\partial z'}+\frac{\partial^2 G^{zz}_{\omega q}}{\partial z\partial z'}\right). \tag{9}$$

Straightforward calculation of the $K_{\omega,q}(z,z')$ gives the following expression:

$$K_{\omega,q}(z,z')=\mathrm{Re}\frac{\omega^2}{2\rho s_l^4 k_l}[e^{ik_l|z-z'|}+R(\omega,q)e^{ik_l(z+z')}], \tag{10}$$

where boundary conditions determine only the reflectance coefficient $R(\omega,q)$. (For the case of a real k_l, R is the reflected-to-incident longitudinal wave amplitude ratio.) For a free surface, we have

$$R(\omega,q)=\frac{4k_lk_tq^2-(k_t^2-q^2)^2}{4k_lk_tq^2+(k_t^2-q^2)^2}, \tag{11}$$

while for a rigid surface, $R(\omega,q)$ takes the form

$$R(\omega,q)=\frac{k_lk_t-q^2}{k_lk_t+q^2}. \tag{12}$$

The normal components of wave vectors for l, t modes (if $q<\omega/s_j$) or the attenuation decrements for these modes (if $q>\omega/s_j$) are introduced by the relations

$$k_j=\begin{cases}\sqrt{(\omega/s_j)^2-q^2}, & q<\omega/s_j \\ i\sqrt{q^2-(\omega/s_j)^2}, & q>\omega/s_j\end{cases}. \tag{13}$$

Note that in accordance with Eq. (3), k_j depends on $\omega+i0$ under calculation of $R(\omega,q)$; by such a substitution, the contribution of Rayleigh waves is described.

III. RELAXATION RATES

In describing relaxation processes in a 2D electron gas it is convenient to consider the losses of the energy and the drift velocity (Q and $\mathbf{U}$) which are introduced by the relations

$$Q=\frac{2}{nL^2}\sum_{\mathbf{p}}\epsilon_p J_{e-\mathrm{ph}}(\mathbf{p}),\quad \mathbf{U}=\frac{2}{nL^2}\sum_{\mathbf{p}}\frac{\mathbf{p}}{m}J_{e-\mathrm{ph}}(\mathbf{p}). \tag{14}$$

Here, n is the concentration of 2D electrons, $\epsilon_p=p^2/2m$, m is the effective electron mass, and $J_{e-\mathrm{ph}}(\mathbf{p})$ is the integral of electron–phonon collisions which is written in the usual form

$$J_{e-\mathrm{ph}}(\mathbf{p})=\sum_{\mathbf{p}'}[W(\mathbf{p}',\mathbf{p})f_{\mathbf{p}'}(1-f_{\mathbf{p}}) -W(\mathbf{p},\mathbf{p}')f_{\mathbf{p}}(1-f_{\mathbf{p}'})], \tag{15}$$

and $f_{\mathbf{p}}$ is the 2D electron distribution function.

To calculate the energy relaxation rate, we assume the electron distribution to be the Fermi function $\tilde{f}_\epsilon=\{\exp[(\epsilon-\mu)/T_e]+1\}^{-1}$ with a chemical potential μ and the temperature T_e differing from the lattice temperature T. Taking into account that the transition probability satisfies the detailed equilibrium condition $W(\mathbf{p}',\mathbf{p})=\exp[(\epsilon'-\epsilon)/T]W(\mathbf{p},\mathbf{p}')$, we obtain

$$Q=\frac{1}{nL^2}\sum_{\mathbf{pp}'}(\epsilon-\epsilon')W(\mathbf{p},\mathbf{p}') \times\left[\exp\left(\frac{\epsilon'-\epsilon}{T}\right)\tilde{f}_{\epsilon'}(1-\tilde{f}_\epsilon)-\tilde{f}_e(1-\tilde{f}_{\epsilon'})\right], \tag{16}$$

where the probability $W(\mathbf{p},\mathbf{p}')$ has a discontinuity at $\epsilon=\epsilon'$, according to Eq. (8). For the case of weak heating ($|T_e-T|\ll T$), Eq. (16) becomes

$$Q=-\nu_e(T_e-T), \tag{17}$$

where the energy relaxation rate, ν_e, is expressed as

$$\nu_e=\frac{2}{n}\int_0^\infty d\epsilon\int_0^\infty d\epsilon'\left(\frac{\epsilon-\epsilon'}{T}\right)^2 W(\epsilon,\epsilon')f_\epsilon(1-f_{\epsilon'}),$$
$$W(\epsilon,\epsilon')=\frac{1}{L^2}\sum_{\mathbf{p},\mathbf{p}'}\delta(\epsilon-\epsilon_p)\delta(\epsilon'-\epsilon_{p'})W(\mathbf{p},\mathbf{p}'). \tag{18}$$

Here, f_ϵ is the Fermi function at equilibrium. Separating out the phonon occupation numbers in $W(\epsilon,\epsilon')$, we can see that the main contributions to ν_e are from the region where $E=(\epsilon+\epsilon')/2\simeq\mu$ and $|\epsilon-\epsilon'|$ is less or of the order of T. The integration over E for the highly degenerate electrons ($T\ll\mu$), may be transformed to

$$\int_0^\infty dE f_{E+\xi/2}(1-f_{E-\xi/2})=\frac{\xi}{e^{\xi/T}-1}, \tag{19}$$

where $\xi=\epsilon-\epsilon'$ is the energy transfer under scattering. As a result, ν_e takes the form

$$\nu_e\simeq\frac{2}{nT^2}\int_0^\mu d\xi\frac{\xi^3 w_e(\xi)}{\cosh(\xi/T)-1}, \tag{20}$$

where the upper limit of integration may be taken to be infinity. Here, $w_e(\xi)$ is expressed through the kernel Eq. (10) according to the relation

$$w_e(\xi)=\frac{Dm^2}{2\pi^2\hbar^5}\int_0^{2\pi}\frac{d\phi}{2\pi}\int dz\,\varphi_z^2\int dz'\,\varphi_{z'}^2 K_{\omega,q}(z,z'), \tag{21}$$

where ϕ is the angle between $\mathbf{p}$ and $\mathbf{p}'$. Let us substitute Eq. (10) into Eq. (21) and introduce the characteristic relaxation rate

$$\overline{\nu}=\frac{(Dp_F)^2 m}{\pi\hbar^4\rho s_l}, \tag{22}$$

where $p_F=\sqrt{2m\mu}$ is Fermi momentum. As a result Eq. (20) is transformed to

$$\nu_e=\frac{\overline{\nu}ms_l^2}{2T^2(s_l p_F)^5}\int_0^{\infty}\frac{d\xi\xi^5}{\cosh(\xi/T)-1}\int_0^{2\pi}\frac{d\phi}{2\pi}\times\int dz\,\varphi_z^2\int dz'\,\varphi_{z'}^2\,\mathrm{Re}\,\kappa_l^{-1}[e^{i\kappa_l p_F|z-z'|/\hbar}+\mathcal{R}e^{i\kappa_l p_F(z+z')/\hbar}], \tag{23}$$

where we have introduced the dimensionless wave vectors $\kappa_j=\hbar k_j/p_F$ and put $\epsilon=\epsilon'=\mu$ in q so that now $q=(2p_F/\hbar)|\sin\phi/2|$. Thus, Eq. (23) contains

$$\kappa_j=\begin{cases}\sqrt{(\xi/p_F s_j)^2-\left(2\sin\dfrac{\phi}{2}\right)^2}, & \left|\sin\dfrac{\phi}{2}\right|<\xi/(2p_F s_j),\\ i\sqrt{\left(2\sin\dfrac{\phi}{2}\right)^2-(\xi/p_F s_j)^2}, & \left|\sin\dfrac{\phi}{2}\right|>\xi/(2p_F s_j),\end{cases} \tag{24}$$

and the reflectance coefficient $\mathcal{R}(k_l,k_t,q^2)$ is transformed to $\mathcal{R}[\kappa_l,\kappa_t,(2\sin\phi/2)^2]$.

Momentum relaxation processes may be analyzed in the same approach by use of the shifted Fermi distribution function, $f_{\mathbf{p}}$. Assuming the anisotropy of this distribution to be weak, i.e., $(\mathbf{pv}_{\mathrm{dr}})\ll T$ where the drift velocity is $\mathbf{v}_{\mathrm{dr}}$, we use

$$f_{\mathbf{p}}\simeq f_\epsilon-(\mathbf{pv}_{\mathrm{dr}})\frac{df_\epsilon}{d\epsilon}. \tag{25}$$

The balance equation for the drift velocity takes the form

$$\mathbf{U}=-\nu_m\mathbf{v}_{\mathrm{dr}}, \tag{26}$$

where the momentum relaxation rate, ν_m, may be expressed by analogy with the above considered energy relaxation case in the form

$$\nu_m=\frac{1}{nL^2}\sum_{\mathbf{pp}'}\frac{[(\mathbf{p}-\mathbf{p}')\mathbf{v}_{\mathrm{dr}}]^2}{Tmv_{dr}^2}W(\mathbf{p},\mathbf{p}')f_\epsilon(1-f_{\epsilon'}). \tag{27}$$

Using Eq. (19) we transform Eq. (27) to

$$\nu_m\simeq\frac{4}{\rho_{2D}T}\int_0^{\mu}\frac{d\xi\xi w_m(\xi)}{e^{(\xi/T)}-1}, \tag{28}$$

where $w_m(\xi)$ differs from Eq. (21) due to the additional angle factor $(1-\cos\phi)$. The expression for ν_m is written as [compare with Eq. (23)]

$$\nu_m=\frac{\overline{\nu}}{2T(s_l p_F)^3}\int_0^{\infty}\frac{d\xi\xi^3}{\cosh(\xi/T)-1}\int_0^{2\pi}\frac{d\phi}{2\pi}(1-\cos\phi)\times\int dz\,\varphi_z^2\int dz'\,\varphi_{z'}^2\,\mathrm{Re}\,\kappa_l^{-1}[e^{i\kappa_l p_F|z-z'|/\hbar}+\mathcal{R}e^{i\kappa_l p_F(z+z')/\hbar}], \tag{29}$$

where κ_j is determined by Eq. (24).

Thus, the calculation of the energy and momentum relaxation rates determined by Eqs. (23) and (29) are reduced to integrations over the energy transfer and the angle $\phi=(\mathbf{p},\hat{\mathbf{p}}')$, and also to averaging over the transverse distribution of the electron density, φ_z^2. These expressions describe the dependencies of the relaxation processes on the temperature and heterostructure's parameters—the electron concentration, the distance between the 2D layer and the surface, and the profile of the confinement potential—and also whether the surface is free or rigid.

IV. REGIMES OF RELAXATION

Let us first discuss the character of the dependencies of the relaxation rates, $\nu_{e,m}$, on the parameters of the heterostructure for the temperature ranges determining by the characteristic temperatures T_0 and T_1; see Eq. (1). These temperatures resolve the following three ranges: high temperatures ($T>T_1$), where the quasielastic relaxation takes place; intermediate temperatures ($T_0<T<T_1$); and low temperatures ($T<T_0$), where the Bloch–Grüneisen regime of inelastic relaxation is realized.

The surface effect on the energy and momentum relaxation processes arises due to the modification of the acoustic field and is as follows: (1) interference between the incident and reflected longitudinal waves ($\omega>s_l q$), (2) reflection induced transformation of an incident transverse wave in a decaying longitudinal wave ($s_t q<\omega<s_l q$), (3) appearance of a Rayleigh wave ($\omega<s_t q$)—in the case of a free surface. These ranges are shown in Fig. 2, where the dimensionless energy transfer $x=|\epsilon-\epsilon'|/T$ and the angle variable $y=|\sin(\phi/2)|$ are introduced. Range 1 corresponds to real values $\kappa_{l,t}$ [given by Eq. (24)], range 2 corresponds to real κ_t and imaginary κ_l, in range 3 both κ_l and κ_t are imaginary. The partial contributions of these additional channels of the scattering depend substantially on the temperature range, the electron concentration, and the distance between the surface and the 2D layer.

For high temperatures, electron energy transfer in the range $\hbar s_l q\ll|\epsilon-\epsilon'|\ll T$ makes the dominant contribution to

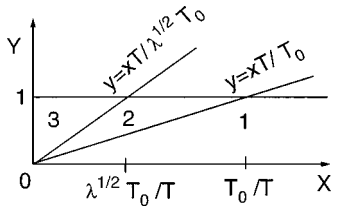

FIG. 2. Three regions of integration in Eqs. (23) and (29). The variables x and y are the dimensionless energy and momentum tranfers: $x=|\epsilon-\epsilon'|/T$, $y=|\mathbf{p}-\mathbf{p}'|/2p_F\leqslant 1$, and $\lambda=(s_t/s_l)^2$.

$\nu_{e,m}$. The relaxation is determined mainly by the quasielastic collisions with equipartition phonons propagating almost perpendicular to the surface. For $k_l \gg q$, we find from Eqs. (11) and (12) the reflectance coefficient $\mathcal{R} \simeq -1$ for a free surface and $\mathcal{R} \simeq +1$ for a clamped surface. As a result, replacing in Eqs. (23) and (29) κ_l with $\xi/p_F s_l$ and $\cosh(\xi/T) - 1$ with $\xi^2/2T^2$, we get

$$\begin{bmatrix} \nu_e \\ \nu_m \end{bmatrix} = 2\overline{\nu}\left(\frac{T}{T_0}\right)^2 \int_{-\infty}^{\infty} dx \begin{bmatrix} Tx^2/2\mu \\ 1 \end{bmatrix} \times \int dz\, \varphi_z^2 \int dz'\, \varphi_{z'}^2 \left[\cos\frac{2T(z-z')x}{T_1 d} \mp \cos\frac{2T(z+z')x}{T_1 d}\right]. \tag{30}$$

Here, $x = \xi/T$, and the parity of the integrands (against x) was used; the upper and lower signs concern to free and rigid surfaces, respectively. In the approach under consideration, the contributions of ranges 2 and 3 are neglected, so that only range 1 may contribute.

The integration of the first term in Eq. (30) (with $z - z'$ argument), gives the bulk values of the relaxation rates, $\nu_{e,m}^b$—for a 2D layer placed far from the surface. The second term, which depends on $z + z'$ argument, describes the surface effect.

For the ground state electron wave function in a rectangular quantum well (QW) with the potential outside taken to be infinite, we obtain from Eq. (30) the known bulk relaxation rates of 2D electrons[6,7] [$\nu_m^b(T)$ proportional T and ν_e^b independent on T] and therewith the surface effect appears to be absent. The latter result is valid for a 2D layer with an arbitrary confinement-potential profile. Indeed, since $\varphi_z(z=0) = 0$, one may consider $z + z' > 0$ under the integration over x, so that $\exp[\pm 2T(z+z')x/T_1]$ vanishes at $x \to \pm i\infty$. Such an integral may be calculated by the residue method and it appears to be zero for an arbitrary function φ_z^2 because the integrand is an analytical function.

Consider now the intermediate temperature range, defined by $T_0 \ll T \ll T_1$. Here the linear connection between κ_j and ξ remains valid, so that $\mathcal{R} = \pm 1$ as above, but now the scattering events become partially inelastic, and one ought to use Planck's phonon distribution. Taking into account that $k_l d \ll 1$, one may simplify Eqs. (23) and (29), replacing z and z' with z_0 in the smooth functions $\exp[i\kappa_l p_F(z \pm z')/\hbar]$. We get

$$\begin{bmatrix} \nu_e \\ \nu_m \end{bmatrix} = 2\overline{\nu}\left(\frac{T}{T_0}\right)^2 \int_0^{\infty} \frac{dx}{\cosh x - 1} \begin{bmatrix} Tx^4/2\mu \\ x^2 \end{bmatrix} (1 \mp \cos\Gamma x), \tag{31}$$

where the dimensionless parameter

$$\Gamma = \frac{4z_0 T}{dT_1}, \tag{32}$$

is proportional to both the temperature T and the QW's position z_0. Using the bulk relaxation rates, $\nu_{e,m}^b$, which follow from Eq. (31) for $z_0 \to \infty$, Eq. (31) can be written as

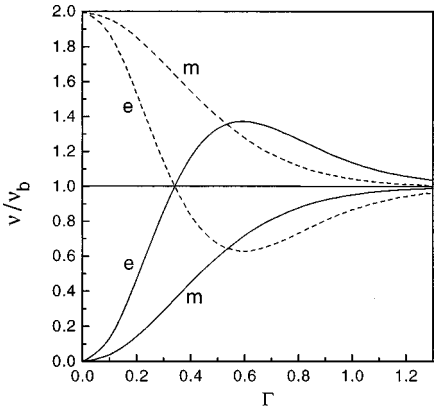

FIG. 3. Energy (e) and momentum (m) relaxation rates, normalized to the bulk values, calculated from Eq. (33) vs the dimensionless parameter Γ, given by Eq. (32). Solid and dashed lines correspond to the free and rigid surfaces.

$$\begin{bmatrix} \nu_e/\nu_e^b \\ \nu_m/\nu_m^b \end{bmatrix} = \int_0^b \frac{dx}{\cosh x - 1} \begin{bmatrix} 15x^4/(8\pi^4) \\ 3x^2/(2\pi^2) \end{bmatrix} (1 \mp \cos\Gamma x). \tag{33}$$

Temperature and position dependencies determined by the integrals Eq. (33) (they may be calculated in an analytical form), are shown in Fig. 3. These dependencies exhibit the effect of the proximity of the surface to the QW, caused by an interference of incident and reflected longitudinal waves (range 1 in Fig. 2), The plotted data give $\nu(T)/\nu^b$ for fixed z_0, or $\nu(z_0)/\nu^b$ for fixed T. In the approach under consideration, the energy of electron–phonon interaction, $D\,\mathrm{div}\,\mathbf{u}$, reduces to Du_z/dz (since $k_l \gg q$) and, due to large acoustic wavelengths ($k_l d \ll 1$) the strong sensibility to the boundary conditions is revealed. At a free surface $du_z/dz = 0$, and in the limiting case of $\Gamma \to 0$ the acoustic phonons scattering are completely suppressed as indicated by the solid curves in Fig. 3 in a vicinity of $\Gamma = 0$. The nonmonotonic behavior of $\nu_e(\Gamma)/\nu^b$ can be explained in the following way. In the calculation of the energy relaxation rate, determined by Eq. (33), the oscillating function $\cos(\Gamma x)$ is integrated together with a function, which has a sharp peak (at $x_m = 3.83$). In a given result, the sign of the surface effect is determined by that of $\cos(\Gamma x_m)$, reflecting the surface-induced appearance of the nodes and antinodes of $D\,\mathrm{div}\,\mathbf{u}$. If $\Gamma x_m > \pi/2$, the effect changes its sign; the value $\Gamma = \pi/2x_m$ is close to the Γ value for which $\nu_e = 0$ in Fig. 3. In the case of ν_m, the corresponding function in Eq. (33) has a maximum at $x = 0$, and $\nu_m(\Gamma)$ appears to be monotonic. Note, that the strong inequality $T_0/T_1 = d(2\pi n)^{1/2} \ll 1$ is possible only for narrow QWs and for low concentrations. For a 3 nm QW, we find that $T_0/T_1 < 0.1$ if $n < 10^{10}\,\mathrm{cm}^{-2}$.

In the low-temperature range, when $T \sim T_0$, with the electron–phonon collisions being substantially inelastic and with the angle-dependent wave vectors, κ_j, of Eq. (24), the relaxation rates are given by cumbersome integrals, and analytical analysis of how the rates depend on T and z_0 can give only rough estimations. For a QW placed close to a surface and for $T \ll T_0$, so that $\Gamma \ll 1$, one may make use of the small-angle scattering approach to obtain

$$\nu^{j}_{e,m}/\nu^{b}_{e,m}=F^{j}_{e,n}(s_l/s_t), \tag{34}$$

where $\nu^b_e \sim T^3$ and $\nu^b_m \sim T^5$ in accordance with the results[3,9,13] for unscreened deformation interaction, and the label $j=f, r$ corresponds to either a free or a rigid surface. The function $F^j_{e,n}$ depends on a ratio s_l/s_t only and does not depend on T. It means that the temperature dependence of the relaxation rates calculated with the phonon modes of semi-infinite medium is the same as that calculated with the bulk modes. For $s_l/s_t=1.73$ we get $F^f_e=2.51$, $F^r_e=1.75$ and $F^f_m=13.2$, $F^r_m=2.37$, with the contribution of the Rayleigh wave exceeding that of the other two mechanisms in about 2 times for ν_e and in about 6 times for ν_m. It should be emphasized, however, that as the temperature T or the distance z_0 increase, the relations Eq. (34) soon breakdown; thus, to estimate the surface effect, one has to turn to numerical calculations.

V. NUMERICAL RESULTS AND DISCUSSION

We have considered a rectangular quantum well and have chosen a ground state wave function of the form $\varphi_z=(2/d)^{1/2}\cos[\pi(z-z_0)/d]$. To extract the surface effect, we calculated the ratio $\nu_{e,m}/\nu^b_{e,m}$, where the normalization functions, $\nu^b_{e,m}$, were determined as $\nu_{e,m}(z_0\to\infty)$. The calculations were carried out for a 3 nm QW, $s_t=4.2\times10^5$ cm/s and the sound velocity ratio $s_l/s_t=1.78$; these values are close to those of InAs and GaAs heterostructures.

The temperature dependencies of the normalized energy and momentum relaxation rates—calculated for the different electron concentrations—are shown in Figs. 4 and 5, where the temperature is measured in degrees Kelvin. The Bloch–Grüneisen temperature T_0 equals 2.65 K for curve 1 and 6.5 K for curve 3. It is seen that the effect of a rigid surface, due to the absence of a Rayleigh wave, is similar to that plotted in Fig. 3 (dashed curves). In the case of a free surface, the behavior of the rates is similar to that presented in Fig. 3 (solid lines) only for the high-temperature wings where the scattering events involving the surface wave become weak. For low temperatures (left-hand side of the plots), the enhancement of the energy and, especially, momentum relaxation rates near a free surface, in comparison with bulk values, is caused primarily by scattering with the Rayleigh wave. The upper boundary of the temperature range where this scattering became dominant coincides approximately with the minima positions of the f curves in Fig. 4 and decreases with the decreasing electron concentration n, and that is in a qualitative agreement with the n dependence of T_0. Note, that even for a small distance ($z_0=3$ nm) and for $T<1$ K, the temperature dependence of the rates ν_e and ν_m differ strongly from dependencies $\nu^b_e(T)$ and $\nu^b_m(T)$.

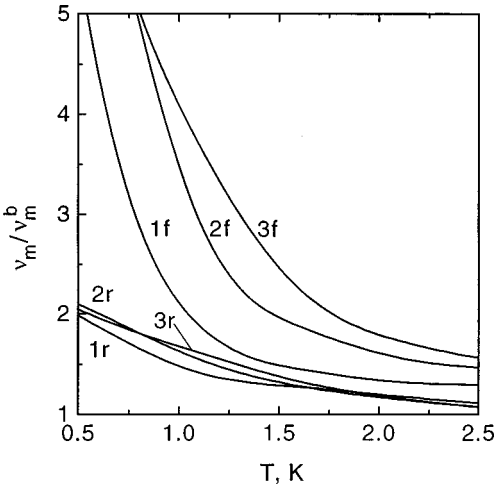

FIG. 5. Momentum relaxation rate, normalized to the bulk value vs temperature for $z_0=3$ nm and n: $1-10^{11}$ cm^{-2}, $2-3\times10^{11}$ cm^{-2}, $3-6\times10^{11}$ cm^{-2}.

In a similar way, one can explain the peculiarities in the QW position which are illustrated in Figs. 6 and 7. It is seen from Fig. 6 that the rigid surface gives rise to a nonmonotonic dependence of ν_e/ν^b_e on position; this dependence is of the same type shown in Fig. 3, where the curves should be considered now as plotted versus the distance z_0 for a fixed T. Comparing, for example, the minima positions of the curves $1r$ and $2r$ (or, with the same result, $3r$ and $4r$) in Fig. 6, we find $z^{1r}_{0\,\min}/z^{2r}_{0\,\min}\simeq3$. This ratio coincides with the

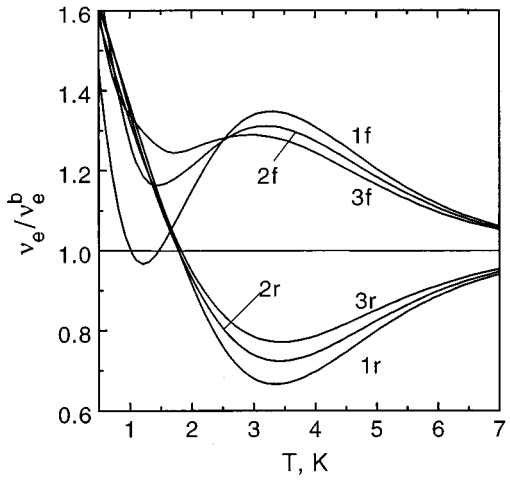

FIG. 4. Energy relaxation rate, normalized to the bulk value vs temperature for $z_0=3$ nm and n: $1-10^{11}$ cm^{-2}, $2-3\times10^{11}$ cm^{-2}, $3-6\times10^{11}$ cm^{-2}.

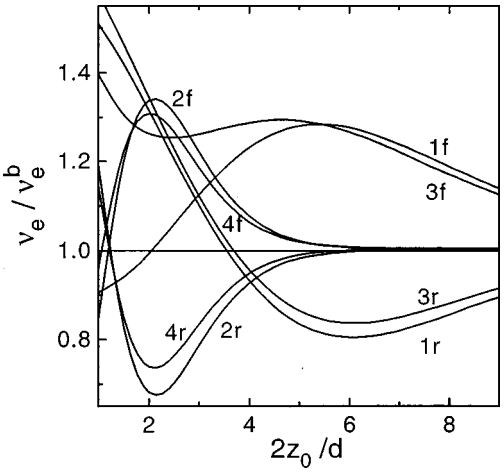

FIG. 6. Energy relaxation rate, normalized to the bulk value vs the distance for T,n: 1–1 K, 10^{11} cm^{-2}; 2–3 K, 10^{11} cm^{-2}; 3–1 K, 3×10^{11} cm^{-2}, 4–3 K, 3×10^{11} cm^{-2}.

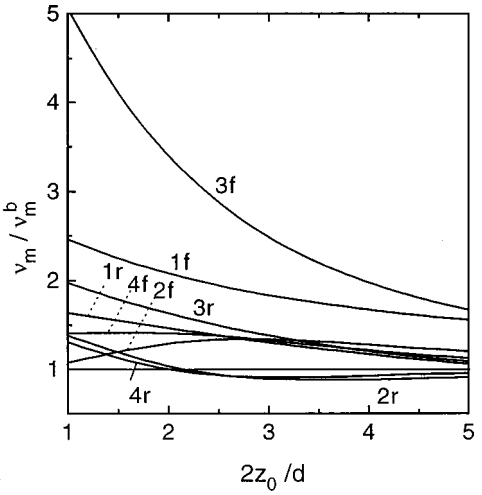

FIG. 7. Momentum relaxation rate, normalized to the bulk value vs the distance for T,n: 1–1 K, $10^{11}\,\mathrm{cm}^{-2}$; 2–3 K, $10^{11}\,\mathrm{cm}^{-2}$; 3–1 K, $3\times10^{11}\,\mathrm{cm}^{-2}$; 4–3 K, $3\times10^{11}\,\mathrm{cm}^{-2}$.

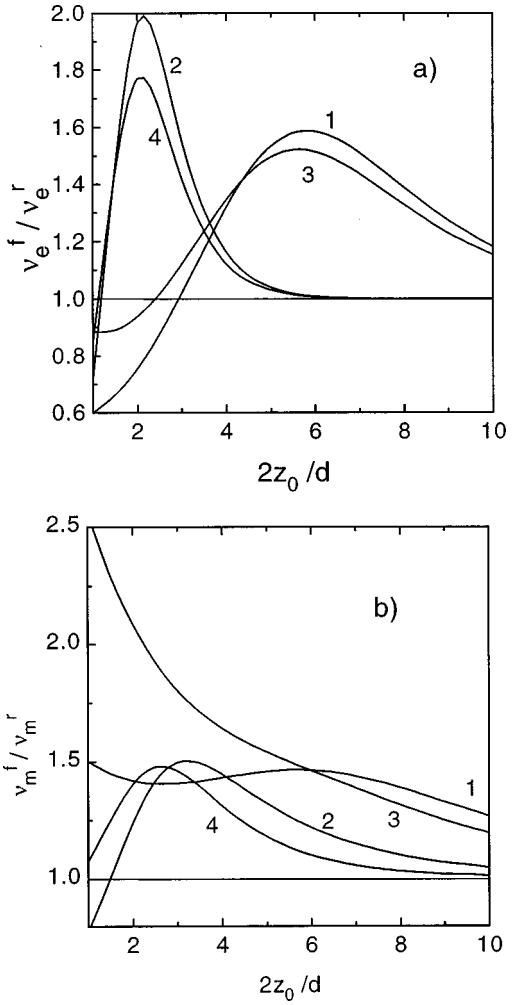

FIG. 8. Ratio of (a) energy and (b) momentum relaxation rates, calculated for the cases of a free and a rigid surface, vs the distance for T,n: 1–1 K, $10^{11}\,\mathrm{cm}^{-2}$; 2–3 K, $10^{11}\,\mathrm{cm}^{-2}$; 3–1 K, $3\times10^{11}\,\mathrm{cm}^{-2}$; 4–3 K, $3\times10^{11}\,\mathrm{cm}^{-2}$.

ratio of the corresponding temperatures: 3 and 1 K. This agrees with T dependence of the minimum of the dashed ''e'' curves in Fig. 3 (remember that Γ is proportional T). The free surface effect, presented in Fig. 6 for higher temperatures (curves $2f$ and $4f$), is also similar to that of Fig. 3; i.e., the surface-induced interference mechanism of scattering dominates here. The curves $1f$ and $3f$, calculated for lower temperature, exhibit the case when scattering is dominated by Rayleigh waves for a QW placed quite near the surface ($z_0 \sim d$). This scattering is greater for QWs with higher electron concentration (compare curves $3f$, $1f$) due to the greater value of the corresponding characteristic temperature T_0. The momentum relaxation rate as a function of z_0 has a less complicated behavior (Fig. 7). In the case of a free surface, in contrary to the functional form presented in Fig. 3 by the solid ''m'' curves, for all values of z_0 we have $\nu_m > \nu_m^b$, which is mainly caused due to interaction with Rayleigh waves. In a structure with a rigid surface, there exist distances for which $\nu_m < \nu_m^b$. This suppression of the relaxation rate appears to be due to the existence of the interference nodes of the electron–phonon interaction: for the case of small angle scattering, realized here, $R<0$ for a rigid, as well as for a free surface.

From Fig. 8 one can see, that the free surface effect exceeds the effect given by a rigid surface. Exceptions appear only for QWs located close the surface (see also the corresponding peculiarities in Fig. 4). The distance, where $\nu_e^f < \nu_e^r$, increases with decreasing T. It should be noted that the dominance of the free surface effect over that of the rigid surface may be rather large.

The key factor governing the dependence of the surface effect on the electron concentration, n, is connected, in the temperature range under consideration, with the concentration dependence of the characteristic temperature T_0. For increasing n, the temperature T_0 increases, and the free surface effect is suppressed for temperatures $T > T_0$; compared with each of the other curves $1f$ and $3f$ in the middle part of Fig. 4 or the same curves in Fig. 5 but for lower temperatures, where electrons undergo an extremely strong interaction with a Rayleigh wave, the influence of the surface is enlarged; as shown by the curves $1f$ and $3f$ in the left-hand side of Fig. 4. The rigid surface effect has a weaker sensitivity due to the absence of the Rayleigh wave. These dependencies are illustrated in Figs. 9 and 10.

Let us list the main assumptions made in these calculations. First, only the deformation potential contribution in electron–phonon interactions has been taken into account. The contribution of the piezoacoustic scattering increases as the temperature decreases.[14,15] According to the results,[14] the temperatures when the contributions of these mechanisms are comparable can be estimated as 2.5 K for GaAs based and 0.6 K for InAs based QWs. Thus, the results presented in this article in a temperature range below these critical values, demonstrate only a pronounced change of the relaxation rates (by a factor of 10 for T of the order of 0.1 K), while for higher temperatures, our calculations provide quantitative results. In addition, the various approaches are related with flat-band approximation which does not describe the effect of the self-consistent electric field (its contribution is small for thin QWs) and by using a simple parabolic energy band (nonparabolic correction factors may be sufficient in InAs-

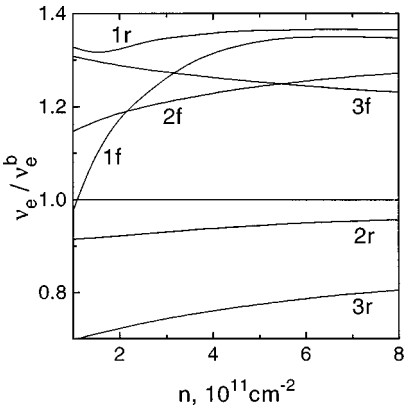

FIG. 9. Energy relaxation rates, normalized to the bulk value, calculated for the cases of a free and a rigid surface, vs the electron concentration for $z_0 = 3$ nm and T: 1–1 K; 2–2 K; 3–4 K.

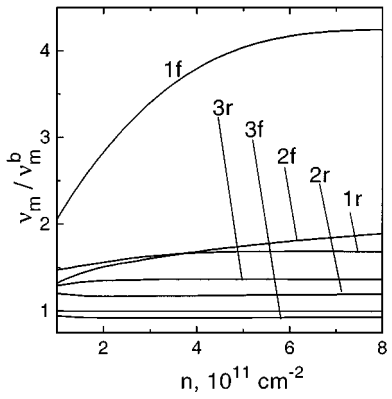

FIG. 10. Momentum relaxation rates, normalized to the bulk value, calculated for the cases of a free and a rigid surface, vs the electron concentration for $z_0 = 3$ nm and T: 1–1 K; 2–2 K; 3–4 K.

based QWs under the concentration near $10^{12}\,\mathrm{cm}^{-2}$). Approximations concerning the methods of calculation have also been made. The exploitation of the balance equations, the corresponding relaxation rates being introduced, is generally accepted and usually gives good agreement with the more advanced methods of the kinetic equation solutions and with the results of Monte Carlo simulation. In deriving Eqs. (23) and (29) the inequality $\mu \gg 2ms_l^2$ has been used; this inequality is well satisfied for degenerate electrons.

VI. CONCLUSIONS

In this article we have presented a systematic study of the modification of the 2D electron energy and momentum relaxation rates occurring due to a near-surface modification of the acoustic field. The electron–phonon deformation interactions are taking into account, and the dependencies on the temperature, position of the 2D electron layer, and the electron concentration are analyzed for the case of degenerate electrons. Numerical calculations demonstrate a *nonmonotonic* character of these dependencies, a severalfold change in the relaxation rates as compared with the bulk values, and a rather strong sensitivity to the 2D electron layer position even for a distance z_0 of the order of 10 times d. In recent years, 2D layers with control over the width of the top layer, including the case of a QW placed just adjacent to the sample boundary based on $In_{0.2}Ga_{0.8}As/GaAs$ heterostructure have been fabricated and investigated by optical methods[16] (this case corresponds to the free surface model). The clamped surface model may be applied to heterostructures with a rigid substrate.

The results presented for these calculations indicated considerable changes (up to 50%–100% under helium temperatures) for the relaxation rates under consideration and they exhibit decrease of their surface-induced modifications, when the QW is removed from the boundary. These results demonstrate that the expressions for $\nu_{e,m}$ under relaxation due to the interaction with the bulk acoustic modes are not suitable for describing experimental data and this failure extends beyond just the case of structures with an ultrathin top layer. Moreover, in a number of publications the deformation potential value had to be adjusted by 50% and even more; see Ref. 3. Since the character of the dependencies on z_0 does not appear to have been investigated experimentally, special measurements are necessary. A special case of interest is the range $T \simeq 1$ K where the surface effect is large; corresponding results, with piezoelectric scatterings included, will be presented separately.[17] Note, that the position dependencies obtained for the energy relaxation rate can substantially change the picture of heat removal processes in semiconductor devices.[18] Decreasing the momentum relaxation rate due to the surface effect in thin (to 5 nm width) QWs gives rise to the possibility of obtaining 2D electron layers with extremely high mobility, limited by the scattering events with structure defects and with roughness of the interfaces, under higher temperatures. Thus, the results presented in this article that are due to near-surface modifications of phonon modes and the consequent changes in the electron–phonon interaction, indicate that *phonon engineering* may be used to substantially modify the relaxation processes in selected quantum-based devices.

ACKNOWLEDGMENTS

The authors are grateful to Dr. M. Stroscio for critical reading of the manuscript and thank Dr. E. Mozdor and Dr. N. Vagidov for assistance in performing the numerical calculations.

[1] H. Ezawa, S. Kawaji, and K. Nakamura, Jpn. J. Appl. Phys. **13**, 126 (1974).
[2] T. Ando, A. Fowler, and F. Stern, Rev. Mod. Phys. **54**, 437 (1982).
[3] H. L. Störmer, L. N. Pfeiffer, K. W. Baldwin, and K. W. West, Phys. Rev. B **41**, 1278 (1990).
[4] M. C. Arican, A. Staw, and N. Balkan, J. Appl. Phys. **74**, 6261 (1993).
[5] A. A. Verevkin, N. G. Ptitsina, K. V. Smirnov, G. N. Gol'tsman, E. M. Gershenzon, and K. S. Ingvesson, JETP Lett. **64**, 404 (1996).
[6] P. J. Price, Ann. Phys. **133**, 217 (1981).
[7] V. Karpus, Sov. Phys. Semicond. **20**, 6 (1986); **22**, 268 (1988).
[8] N. A. Bannov, V. A. Aristov, V. V. Mitin, and M. A. Stroscio, Phys. Rev. B **51**, 9930 (1995).
[9] S. M. Badalyan and I. B. Levinson, Sov. Phys. Solid State **30**, 1592 (1988).
[10] S. M. Badalyan, Sov. Phys. Semicond. **23**, 1087 (1989).
[11] A. Knäbchen, Phys. Rev. B **55**, 6701 (1997).
[12] V. I. Pipa, F. T. Vasko, and V. V. Mitin, Phys. Status Solidi B **204**, 234 (1997).

[13] A. A. Maradudin and D. L. Mills, Ann. Phys. (N.Y.) **100**, 262 (1976).
[14] P. J. Price, J. Appl. Phys. **53**, 6863 (1982).
[15] V. Karpus, Semicond. Sci. Technol. **5**, 691 (1990).
[16] J. Dreybrodt, A. Forchel, and J. P. Reittmaier, Phys. Rev. B **48**, 14741 (1993).
[17] To account simultaneously for the deformation and piezoelectric interactions, it is not enough to add the corresponding contribution to the collisions integral, one must also consider an interference of these mechanisms (see F. T. Vasko and V. V. Mitin, *Proceedings of the Third International Symposium on Quantum Confinement: Physics and Applications* (Electrochemical Society, Chicago, 1995), Vol. 95-17, p. 197; where an interference between the usual deformation potential and the contribution of the heteroboundary vibrations has been considered).
[18] V. V. Mitin, N. A. Bannov, G. Paulavicius, and M. A. Stroscio, *Proceedings of the Semiconductor Device Modeling Workshop* (NASA Ames Research Center, Moffett Field, CA, 1996), pp. 160–172.